

Experimental and Theoretical Study of Gold(III)-Catalyzed Hydration of Alkynes

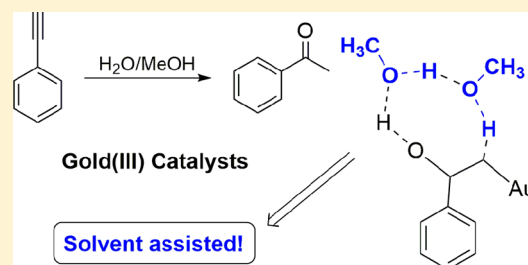
Jesús Cordón,[†] Gonzalo Jiménez-Osés,[‡] José M. López-de-Luzuriaga,^{*,†} Miguel Monge,[†] M. Elena Olmos,[†] and David Pascual[†]

[†]Departamento de Química, Centro de Investigación en Síntesis Química (CISQ), Complejo Científico-Tecnológico, Universidad de La Rioja, 26004 Logroño, Spain

[‡]Department of Chemistry and Biochemistry, University of California, Los Angeles, California 90095, United States

S Supporting Information

ABSTRACT: The properties of different Au(III) halo dithiocarbamate complexes of structure $[\text{AuX}_2(\text{S}_2\text{CN}(\text{R})_2)]$ as suitable catalysts for the hydration reaction of phenylacetylene have been tested. Moderate catalytic activity was found for $\text{X} = \text{Cl}, \text{Br}$, while those compounds in which $\text{X} = \text{I}, \text{C}_6\text{F}_5$ are inert. A working mechanism involving the initial dissociation of a labile ligand (Cl or Br) followed by coordination and activation of the alkyne, solvent-assisted attack of water, and enol tautomerization has been proposed through computational studies.



INTRODUCTION

In the field of homogeneous catalysis, the use of gold complexes as catalysts for organic reactions is an area of permanent interest that has led to the discovery of new reaction pathways able to reduce the number of steps required for many organic syntheses.^{1–4} Among them, the catalyzed hydration of alkynes⁵ is a benchmark reaction for chemical sustainability in the production of downstream derivatives, since it provides an environmentally friendly and safe route for the formation of C–O bonds from hydrocarbons, leading to high-value materials for the chemical industry such as ketones and aldehydes.

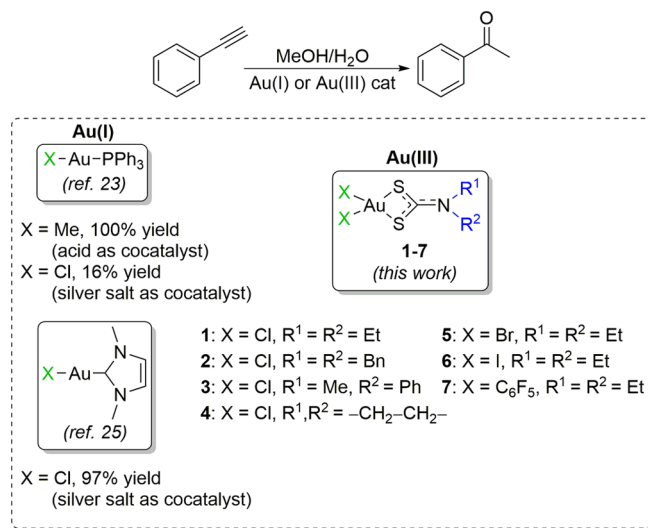
In the past, the most extensively employed catalytic systems for this reaction consisted of toxic mercury salts in acidic media,^{6,7} although other less harmful (but expensive) transition-metal-complex catalysts containing Rh^8 or Pt^9 have also been described. Gold compounds in small amounts are known to be effective catalysts in the addition of nucleophiles to triple bonds.¹⁰ Au(I) catalysts have been more extensively used in these types of transformations^{11–15} than Au(III) species.^{16,17} The main reason for this trend is that Au(I) complexes are usually more stable than those of Au(III), in spite of the fact that the latter is isoelectronic with well-known catalytic centers such as Pt(II), Pd(II), Rh(I), and Ir(I).

In this context, compounds of the types $[\text{Au}(\text{PR}_3)]^+$ ($\text{R} = \text{alkyl}, \text{aryl}$)¹⁸ and $[\text{Au}(\text{NHC})]^+$ ($\text{NHC} = \text{N-heterocyclic carbene}$)^{19–21} have been extensively used for the hydration of alkynes, with progressive improvement of the catalyst efficiency and reaction conditions over the years. For instance, earlier studies by the groups of Teles²² and Tanaka¹⁰ reported the use of $[\text{AuMe}(\text{PPh}_3)]$ in acidic media, leading to CH_4 release upon heating and formation of $[\text{Au}(\text{PR}_3)]^+$ as the active species. It has been proposed that both the Au(I) fragment and excess acid act as cocatalysts. The same catalytic system $[\text{AuMe-}$

$(\text{PPh}_3)]/\text{H}_2\text{SO}_4$ was tested by Laguna and co-workers for the hydration of phenylacetylene in refluxing aqueous solutions,²³ achieving a high conversion to acetophenone (Scheme 1). The same reaction was carried out by generating the active $[\text{Au}(\text{PR}_3)]^+$ catalyst in situ from $[\text{AuCl}(\text{PR}_3)]$ upon addition of a silver salt. In this case the conversion to acetophenone was lower, probably due to the absence of an acid cocatalyst.

In a recent report Corma et al.²⁴ have shown that an isolated Au(I) complex bearing the weakly coordinating bis-

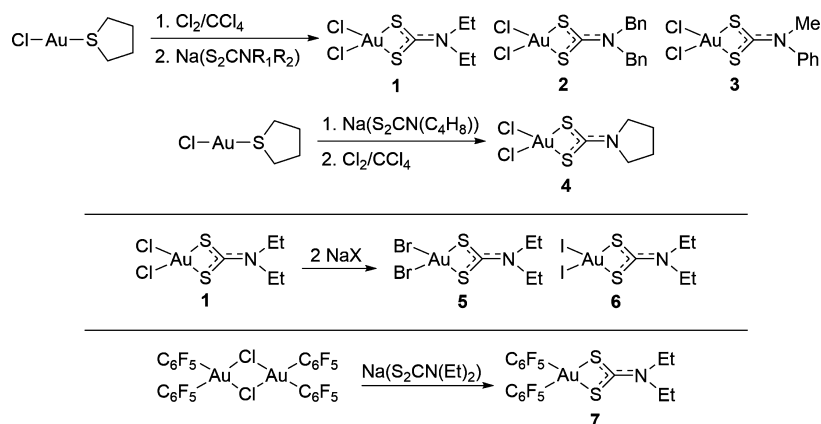
Scheme 1. Hydration of Phenylacetylene



Received: May 15, 2014

Published: July 16, 2014

Scheme 2. Synthesis of Au(III)–Dithiocarbamate Catalysts



(trifluoromethanesulfonyl)imidate (NTf₂[−]) ligand, [Au(NTf₂)(PR₃)], catalyzes the hydration of substituted alkynes at room temperature without acid promoters.

Nolan et al. demonstrated that Au(I) carbene cationic species such as [Au(NHC)]⁺, derived from [AuCl(IPr)] (IPr = *N,N'*-bis(2,6-diisopropylphenyl)imidazol-2-ylidene) in the presence of AgSbF₆, is an excellent catalyst for the addition of water to alkynes that operates at very low catalyst loadings and under acid-free conditions.²⁵

From a theoretical perspective, recent DFT studies have shown that the mechanism for the hydration of alkynes using Au(I) catalysts is better explained when solvent molecules are taken into account, leading to lower reaction barriers and more efficient proton transfer in comparison to those in the gas-phase environment without solvent molecules.^{26,27}

At this point, it is worth mentioning that from the first studies to the more recent ones a clear sophistication in the rational design of the Au(I) catalyst for the hydration of alkynes and the explanation of the mechanism of catalysis can be observed, which is directly related to milder and more selective methodologies.

However, only few Au(III) complexes have been used as catalysts for this transformation. Utimoto et al. described the use of Na[AuCl₄]²⁸ as a catalyst for the addition of water and alcohols to alkynes in good yields. Also, several aryl-substituted (mesityl or pentafluorophenyl) Au(III) anionic or neutral organometallic complexes have been described as catalysts for the hydration of phenylacetylene.²³ In this case the authors proposed a mechanism for the addition of water to the alkyne catalyzed by the neutral dimer [Au(C₆F₅)₂Cl]₂, including a collateral reductive elimination pathway to explain the observed formation of metallic gold.

However, as Teles recently pointed out,²⁹ “the question of how Au(III) complexes catalyze the addition of water to alkynes is still unanswered.” To the best of our knowledge, there have been no theoretical studies on the mechanism of the hydration of alkynes using Au(III) catalysts.

We aimed to fill in this gap by performing an experimental and theoretical study of this prototypical reaction using a well-known type of Au(III) species. As described previously,³⁰ Au(III) halo complexes bearing bidentate S,S-donor ligands show good chemical and thermal stability, the Au–X or Au–S bonds being sufficiently labile to permit substitutions by other groups, which is a necessary event for catalysis. We therefore studied the behavior of different Au(III) dithiocarbamate compounds of the [AuX₂(dtc)] stoichiometry (X = Cl, Br, I;

dtc = S₂CNEt₂ (1, 5–7), S₂CNBn₂ (2), S₂CN(Me)Ph (3), S₂CN(pyrrolidine) (4)) in the hydration reaction of phenylacetylene (Scheme 1). Hence, we report in this paper the experimental results obtained with Au(III) catalysts 1–7 in the hydration reaction of phenylacetylene, together with a thorough theoretical study of two possible hydration mechanisms, involving the dissociation of either the Au–X or Au–S bonds.

RESULTS AND DISCUSSION

Synthesis and Characterization of the Catalysts.

Complexes 1–3 were prepared by oxidation of [AuCl(tht)] (tht = tetrahydrothiophene) with an excess of Cl₂ in CCl₄ solution, followed by displacement of the tht ligand with the corresponding dithiocarbamate sodium salt in acetone (compound 1) or dichloromethane (compounds 2 and 3). Compound 4 was prepared in a similar manner, but the tht–dithiocarbamate ligand exchange was carried out prior to oxidation of the Au(I) center with Cl₂. Compounds 5 (X = Br) and 6 (X = I) were prepared by reaction of complex 1 with the appropriate halogen salt, NaX, in a mixture of dichloromethane and water. Finally, compound 7 (X = C₆F₅) was prepared by reaction of the dimeric complex [Au(C₆F₅)₂Cl]₂ with the corresponding sodium salt of dithiocarbamate Et₂NCS₂[−] in acetone (see Scheme 2 and the Experimental Section).

The formation of the expected complexes and coordination of the dithiocarbamate ligands to the gold center was verified by ¹H NMR and IR spectroscopy (see the Experimental Section). The ¹⁹F NMR spectra of compound 7 shows the signals corresponding to the C₆F₅ group at −122.1 (F_{ortho}), −158.5 (F_{para}), and −163.2 ppm (F_{meta}), which are commonly found in Au(III)–C₆F₅ species.³¹

The coordination of dithiocarbamate ligands to the Au(III) center was also verified by the presence of characteristic ν(C–N) and ν(CS₂) IR bands.³² Also, in compounds 1–4 characteristic ν(Au(III)–Cl)³³ bands appear, as well as typical bands of C₆F₅ groups³⁴ in compound 7 (see the Experimental Section).

X-ray Structural Determination of Compound 2. Single crystals suitable for X-ray diffraction studies of complex 2 were obtained by slow diffusion of hexane into a saturated solution of the complex in dichloromethane. The crystal structure of complex 2 contains discrete molecules in which a tetracoordinated Au(III) center, which lies in the 2-fold axis, is surrounded by two chlorine atoms and both sulfur atoms of a dibenzylidithiocarbamate ligand in a cis disposition (see Figure 1). The geometry at gold is essentially square planar (Cl–Au–

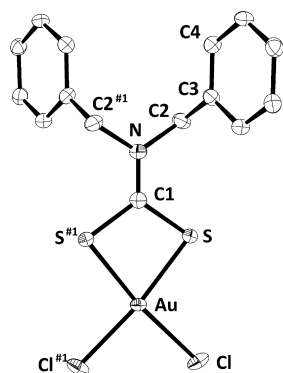


Figure 1. Molecular structure of compound **2** with the labeling scheme for the atom positions. Hydrogen atoms are omitted for clarity and ellipsoids are drawn at the 30% level. Selected bond lengths (Å) and angles (deg): Au–S 2.3005(14), Au–Cl 2.3116(15), S–C(1) 1.745(5), C(1)–N 1.299(10), N–C(2) 1.491(7), S–Au–Cl#1 172.65(6), S#1–Au–S 76.65(7), Cl–Au–Cl#1 91.29(9), N–C(1)–S 125.2(2), S–C(1)–S#1 109.6(4). Symmetry transformation: (#1) $-x + 1, y, -z + 3/2$.

Cl 91.29(9)°, although somehow distorted as a consequence of the restricting chelate angle of the dithiocarbamate ligand (S–Au–S 76.65(7)°). This angle lies within the range found in a total of 73 entries in 38 crystal structures containing the fragment $[\text{Au}(\mu\text{-S}_2\text{CN})]$, which vary from 65.71(5)° in $[\text{Au}(\text{PPh}_3)_2\{\mu\text{-S}_2\text{CN}(\text{i-Pr})_2\}]^{35}$ to 78.6(3)° in $[\text{Au}(\text{o-C}_6\text{H}_4\text{CH}_2\text{NMe}_2)(\mu\text{-S}_2\text{CNMe}_2)]\text{BPh}_4^{36}$ (mean value of 74.85°).

The Au–Cl bond length of 2.3116(15) Å is slightly long for a gold(III) complex, which could favor the displacement of the Cl by the corresponding alkyne in the catalytic process (*vide infra*). This is due to the strong trans influence of the S donor ligands and is of the same order as the Au–Cl bond distances found in the related dithiocarbamate complex $[\text{AuCl}_2\{\mu\text{-S}_2\text{CN}(\text{EtOH})_2\}]$ (2.316(3) and 2.325(3) Å)³⁷ or in other compounds containing the fragment $[\text{AuCl}_2(\mu\text{-SCS})]^{38-40}$ but significantly shorter than in $[\text{AuCl}_2\{\mu\text{-S}_2\text{C}=\text{C}\{\text{C}(\text{O})\text{Me}\}_2\}]$ (2.3491(13)–2.3662(13) Å).⁴¹

The Au–S bond length of 2.3005(14) Å in **2** is nearly identical with the mean value of 2.3038 Å found in complexes of the type $[\text{AuX}_2(\text{dtc})]$ (X = Cl, Br), in which the Au–S bond distances vary from 2.287(3) Å in $[\text{AuCl}_2\{\mu\text{-S}_2\text{CN}(\text{EtOH})_2\}]^{27}$ to 2.319(2) Å in $[\text{AuBr}_2\{\mu\text{-S}_2\text{CN}(\text{Me})(\text{CH}_2\text{CO}_2\text{Et})\}]^{42}$. It also compares well with those observed in the $[\text{AuCl}_2(\mu\text{-SCS})]^{37-41}$ complexes cited above, in which the Au–S distances range from 2.273 Å in $\text{NBu}_4[\text{AuCl}_2\{\mu\text{-S}_2\text{C}=\text{C}(\text{CN})(\text{CO}_2\text{Et})\}]^{38}$ to 2.305(3) Å in $[\text{AuCl}_2\{\mu\text{-S}_2\text{CN}(\text{EtOH})_2\}]^{37}$.

Finally, the angles around the central C atom of the dibenzylidithiocarbamate ligand in compound **2** (see Figure 1) are consistent with sp^2 hybridization, although the S–C–S angle (109.6(4)°) is narrower than that expected for this hybridization because of the behavior of the ligand as chelate. A comparison of both types of C–N bond lengths (C(1)–N 1.299(10) Å, C(2)–N 1.491(7) Å) is in accordance with a certain double-bond character in the former.

Hydration of Alkynes: Experimental Study. After preparing and characterizing compounds **1–7**, we tested their catalytic capabilities in the hydration reaction of phenylacetylene in refluxing aqueous methanol. The results of these experiments are shown in Table 1.

The catalytic tests performed with compounds **1–4** (Table 1, entries 1–5) showed that complex **1** is modestly active (46%

Table 1. Results of Catalytic Tests with Au(III) Dithiocarbamate Complexes **1–7**

entry	cat.	cat. loading (mol %)	additive (10 equiv)	conversn (%) ^a
1	1	2		25
2	1	4		46
3	2	2		18
4	3	2		11
5	4	2		10
6	5	2		26
7	6	2		0
8	7	3		0
9	1	2	NaOH	0
10	-		HB F_4	0
11	1	2	HB F_4	46
12	1	4	HB F_4	98
13	1	4	AgOTf (1 equiv)	0

^aConversion to acetophenone determined by GC–MS.

conversion in 90 min) in moderate catalyst loading (4 mol %). A reduction of the amount of catalyst **1** to 2 mol % reduced its activity in the same proportion (25% conversion). Meanwhile, complexes **2–4** were less active under the latter conditions (10–18%). This first set of results shows that the nature of the S-donor ligand has little effect on the performance of the catalyst.

We then studied the effect of substituting the halogen ligand in compound **1** (Table 1, entries 6–8). The results show that the replacement of chlorine by bromine does not affect conversion, while the substitution by iodide or C_6F_5 groups completely shuts down the reactivity.

In addition, we tested the effect of the solvent on the reaction yield (see Table S1 of the Supporting Information). The results suggest the requirement of a protic solvent (acetonitrile gives a conversion of 0%) and a solvent of small size (the conversion with isopropyl alcohol was 8%), such as methanol (46%), due to the need for participation of the solvent as an assistant molecule in the key steps of the catalytic cycle (*vide infra*).

Finally, we tested the effect of adding acid and basic cocatalysts in a 1:10 molar ratio with respect to the catalyst (Table 1, entries 9–12). The addition of NaOH shuts down the reaction by decomposing the catalyst, while in the presence of HBF_4 , the reactant conversion is doubled, achieving complete conversion when 4 and 40 mol % of catalyst and acid are used, respectively. This finding suggests that the presence of acid might be involved in some crucial step of the operating catalytic cycle. The addition of silver triflate as cocatalyst, as is used in other catalytic processes in a 1:1 molar ratio with respect to the catalyst (Table 1, entry 13), causes the immediate decomposition of the catalyst by initial formation of $\text{Ag}(\text{S}_2\text{CNET}_2)$ and AuCl and immediate Au(0) formation.

In view of these results, two opposing factors seem to be related to the catalytic properties of the different complexes tested. On the one hand, the electrophilicity of Au(III) is reduced, following the expected trend, attending to the electronegativity of each ligand ($\text{Cl} \approx \text{C}_6\text{F}_5 > \text{Br} > \text{I}$), as reflected in the NBO charges for the Au(III) atom summarized in Table 2. On the other hand, the aptitudes of each ligand as a leaving group are reduced in the opposite way ($\text{I} > \text{Br} > \text{Cl} > \text{C}_6\text{F}_5$), as demonstrated by the Au–X bond dissociation energies (BDE; see Computational Details) shown in Table 2. Overall, these results suggest the importance of creating a coordination vacancy in the metal for the reaction to proceed.

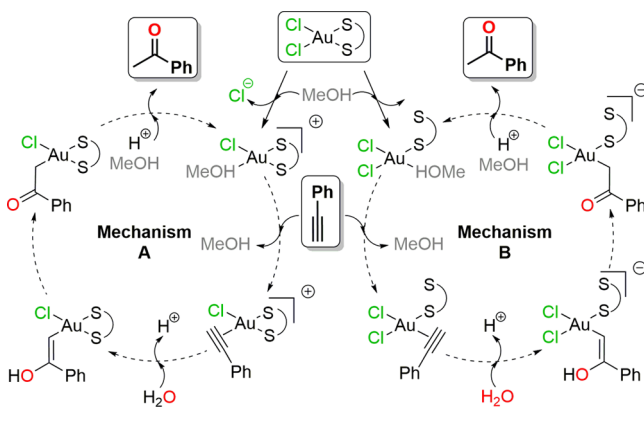
Table 2. NBO Charges and Au–X Bond Dissociation Energies (BDE) Calculated at the M06-2X Level for the Au(III) Atom in Compounds 1 and 5–7

compd	Au NBO charge (e)	Au–X BDE (kcal mol ⁻¹)
1 (X = Cl)	0.33	152.4
5 (X = Br)	0.18	148.8
6 (X = I)	-0.03	144.4
7 (X = C ₆ F ₅)	0.39	187.1

We also studied this type of reaction with different alkynes (see Table S2 in the Supporting Information) such as 1-hexyne (alkyl substituted), 1-phenyl-1-propyne (alkyl, aryl substituted), and diphenylacetylene (diaryl substituted). We found similar results for 1-hexyne and very low or no conversions for the case of nonterminal alkynes (with diphenylacetylene as substrate the conversion was 0%). This trend is probably due to the steric hindrance exerted by the substituents in the activation of the triple bond by the metal center or in the O-nucleophilic approach, steps that require greater hollow space.

We envisioned two possible mechanisms for the hydration of phenylacetylene catalyzed by dithiocarbamate Au(III) complexes (Scheme 3). In mechanism A, the coordination vacancy

Scheme 3. Proposed Catalytic Cycles for the Au(III)-Catalyzed Hydration Reaction of Phenylacetylene



in Au(III) necessary to maintain the square-planar geometry and facilitate catalysis along the reaction pathway is generated by the departure of one chloride ligand.

On the other hand, in mechanism B, the dithiocarbamate ligand isomerizes from bidentate to monodentate to create the necessary coordination site.

Hydration of Phenylacetylene: Theoretical Study. We have carried out a thorough computational study of the two proposed catalytic cycles for the hydration of phenylacetylene catalyzed by the most active Au(III) catalyst [AuCl₂(S₂CNEt₂)] (1) (see Computational Details). A good agreement was obtained between the optimized structure of compound 1 and the X-ray diffraction structure of compound 2 (see Table S3 in the Supporting Information).

Figure 2 shows the minimum-energy pathways calculated at the DFT/M06-2X level for both mechanisms. In an initiation step preceding catalysis, the catalyst (int1) is activated by replacement of one anionic ligand (either Cl or one of the coordinating S atoms of dtc) by one solvent molecule (methanol) to produce the cationic (int3-A) or neutral (int3-B) Au(III) active species for mechanisms A and B, respectively.

Mechanism A: Dissociation of Chloride Ligand. In this pathway, the catalytic cycle is started by the substitution of methanol by phenylacetylene, which involves a quite high activation barrier of ca. 31 kcal mol⁻¹ (ts4-A, transition state not located for mechanism B). Au– π interactions are quite strong in this intermediate, as reflected by the short Au–C distance (2.4 Å) and the loss of linearity of the phenylacetylene moiety (164°). Overall, this first step of the catalytic cycle is endergonic by 20.8 kcal mol⁻¹.

The next step involves the hydration of the predistorted alkyne by addition of one water molecule to the internal position of the triple bond (ts5-A, Markovnikov regioselectivity), which corresponds to the only product observed experimentally. After testing different possibilities (Figure S1 and Table S4 in the Supporting Information), we found that this nucleophilic attack is assisted by two molecules of solvent (methanol) (Figure 3), which contribute to reduce the intrinsic activation barrier from 13.4 to 11.5 kcal mol⁻¹. These solvent molecules activate the water molecule, stabilize the positive charge developed in the oxygen atom upon nucleophilic attack, and help to deprotonate the adduct. Even so, this transition state is the highest point in the whole potential energy surface (PES), with a quite high activation energy of 32.3 kcal mol⁻¹. However, this step benefits the thermodynamics of the reaction, which so far had been continuously uphill, yielding a slightly exergonic process ($\Delta G = -2.4$ kcal mol⁻¹) with respect to the reactants, in which a neutral Au(III) alkylidene intermediate (int5-A) is formed.

The next step is the solvent-assisted tautomerization of Au(III)-alkylidene int6-A, from its enol to the corresponding keto form (int8-A). Among the different possibilities tested (see Figure S2 and Table S5 in the Supporting Information), the assistance of two solvent molecules (methanol) (Figure 4, left panel) dramatically decreases the activation barrier (ts7-A) from 45.9 to 14.6 kcal mol⁻¹. These results reinforce the importance of solvent effects in catalytic processes in which proton transfer steps are involved and stress the need of including explicit solvent molecules in the calculations to properly model these reactions.²⁶ This step is quite exergonic, yielding a very stable Au(III) alkyl complex (int8-A), which can be considered also a C-enolate, as the resting state of the catalytic cycle ($\Delta G = -19.4$ kcal mol⁻¹ with respect to the reactants).

For the last step of the catalytic cycle we proposed the methanol-assisted protonation of the enolate (Figure 4, right panel) because it releases acetophenone and regenerates the catalyst in its solvated cationic active form (int3-A), ready to start the next catalytic cycle. In addition, it displays a very low activation energy that would be related to the great importance of the acid cocatalyst in the phenylacetylene to acetophenone conversion. Overall, the hydration of acetylene catalyzed by [AuCl₂(S₂CNEt₂)] (1) is exergonic by -35 kcal mol⁻¹.

Mechanism B: Partial Dissociation of Dithiocarbamate Ligand. This alternative pathway differs from mechanism A only in the first step, in which the dissociation of one Au–S bond creates the coordination site for phenylacetylene. As can be seen in Figure 2, this pathway is always less favorable than mechanism A due to the higher activation barrier associated with the Au–S dissociation, which is ~15 kcal mol⁻¹ higher than the cleavage of the Au–Cl bond. These results are consistent with the well-documented aurophilicity of dithiocarbamates⁴³ and might also reflect the beneficial effect of fully

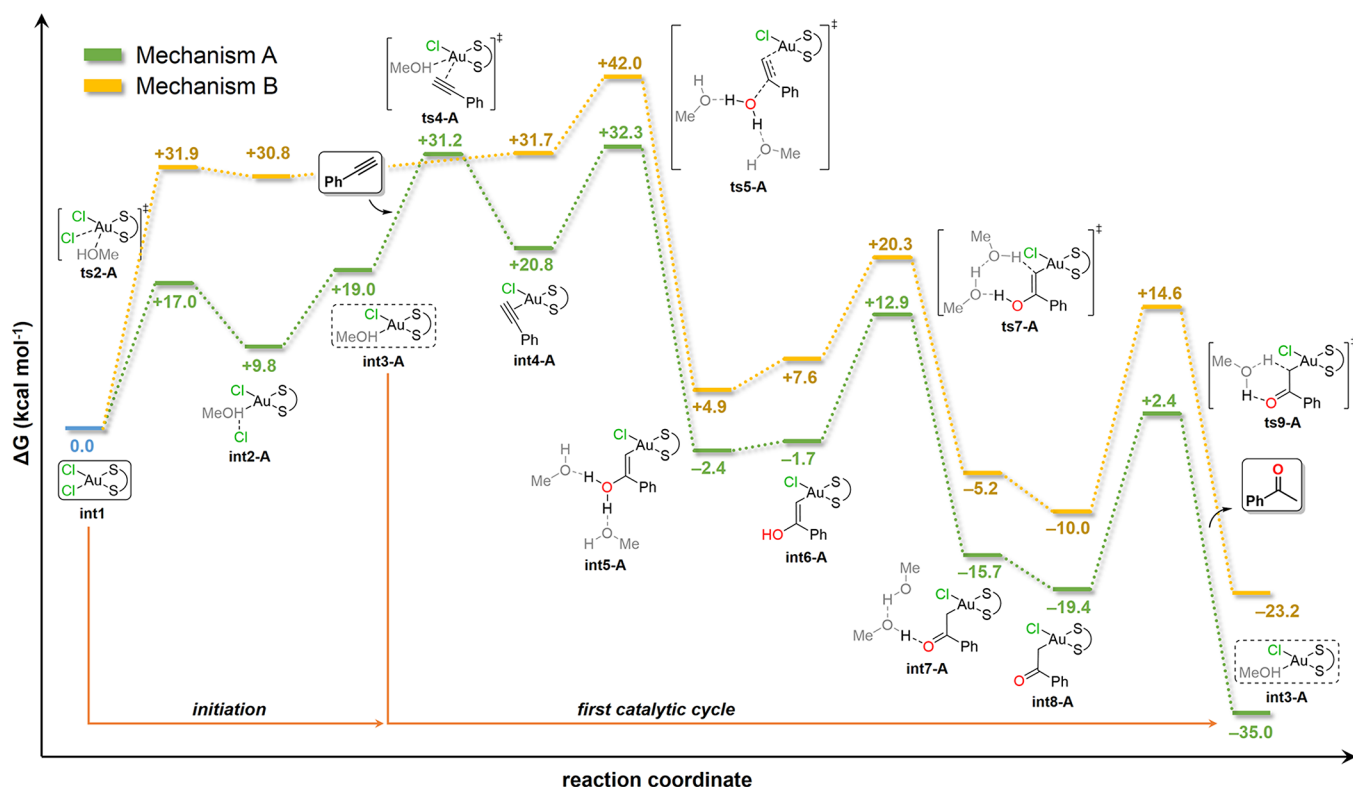


Figure 2. Complete minimum-energy reaction pathway calculated for mechanisms A and B at the M06-2X/SDD level. Relative Gibbs free energies (ΔG) are given in kcal mol^{-1} .

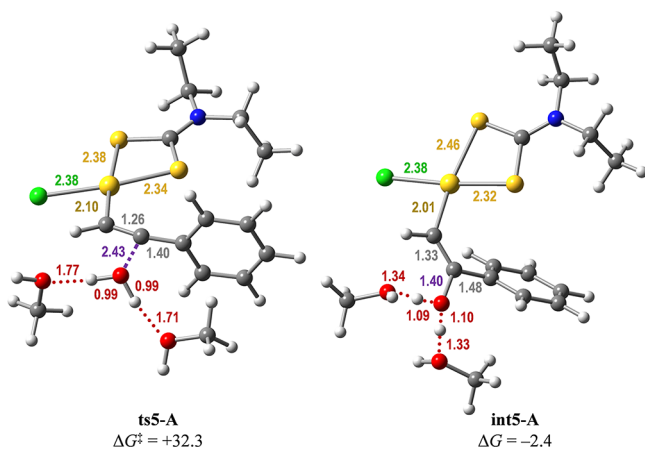


Figure 3. Solvent-assisted nucleophilic attack of water to phenylacetylene (mechanism A). Free energies (ΔG) are given in kcal mol^{-1} .

dissociating a monodentate anionic ligand such as Cl, which becomes greatly solvated in water.

The rest of the catalytic cycle shows essentially the same energy profile, with very similar stationary points along the PES, which is systematically 8–12 kcal mol^{-1} higher in energy than mechanism A. Figure 5 shows the geometries of the nucleophilic hydration (**ts5-B**) and tautomerization steps (**ts7-B**) calculated for this mechanism.

CONCLUSIONS

The properties of different Au(III) halo dithiocarbamate complexes as suitable catalysts for the hydration reaction of phenylacetylene have been tested. A moderate activity was observed for some of them using reasonable catalyst loading

(2–4% mol), whereas quantitative formation of acetophenone is detected when an acid cocatalyst was used.

The structure of the dithiocarbamate group does not affect the activity of these compounds, but the nature of the labile ligands determines their proficiency as catalysts. Hence, electronegative and good leaving groups such as Cl and Br facilitate turnover, but electropositive or very coordinating ligands such as I and C_6F_5 do not.

A detailed computational study of two different pathways for the reaction allowed us to propose the dissociation of the halide ligand as the initiation step of the most favored mechanism, while the strong bidentate coordination of the dithiocarbamate ligand is maintained throughout the whole catalytic cycle. Solvent effects have been revealed to be important to decrease the activation barriers of both the nucleophilic attack of water and the tautomerization of the corresponding Au(III) alkylidene enol intermediate.

From a theoretical viewpoint, the solvent-assisted study of the mechanism of hydration of alkynes using Au(III) complexes as catalyst has given rise to satisfactory results. Thus, a more efficient proton transfer and less energetic barriers in comparison to gas-phase calculations have been obtained. This result completes the previous Hashmi's report about hydration of alkynes catalyzed by Au(I) complexes.^{26,27}

While these stable Au(III) dithiocarbamate complexes have been less used in catalysis than Au(I) complexes, their unique features in terms of geometry and electronic properties offer new opportunities for reactivity that we will continue to explore in different reactions.

EXPERIMENTAL SECTION

General Procedures. The compounds $[\text{AuCl}(\text{tht})]^{44}$ and $[\text{Au}(\text{C}_6\text{F}_5)_2\text{Cl}]^{45}$ were synthesized according to published procedures.

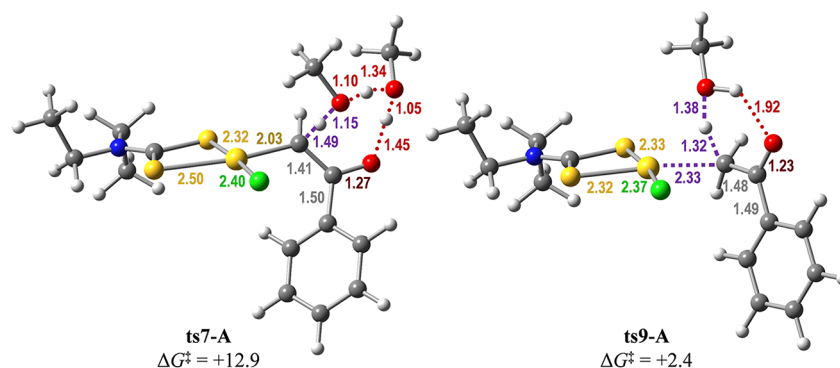


Figure 4. Solvent-assisted enol–keto tautomerization (left) and final protonation (right) to release acetophenone (mechanism A). Free energies (ΔG) are given in kcal mol⁻¹.

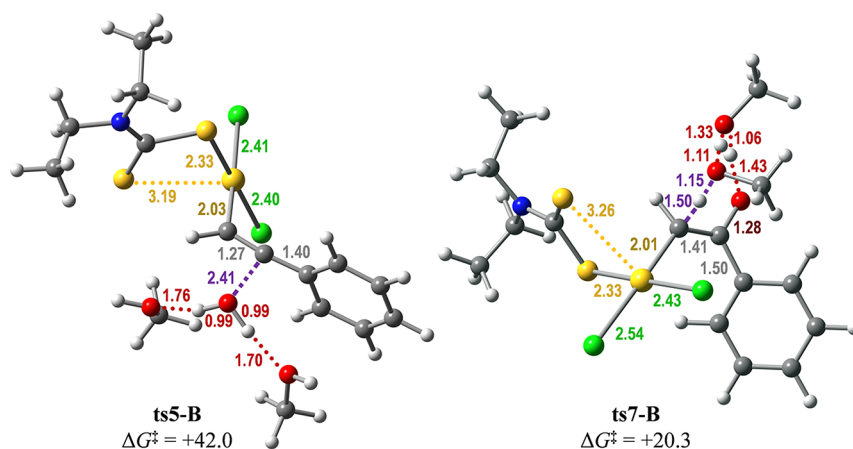


Figure 5. Solvent-assisted nucleophilic attack of water to phenylacetylene (left) and enol–keto tautomerization (right) (mechanism B). Free energies (ΔG) are given in kcal mol⁻¹.

NaS₂CNEt₂ and NaS₂CN(pyrrolidine) were purchased from Aldrich, while NaS₂CNBn₂ was acquired from TCI Europe. NaS₂CN(Me)Ph was prepared as previously reported.⁴⁶ Infrared spectra were recorded in the 4000–220 cm⁻¹ range on a Nicolet Nexus FT-IR with CsI beam splitter, using Nujol mulls between polyethylene sheets. C, H, N, and S analyses were carried out with a PerkinElmer 240C microanalyzer. MALDI-TOF spectra were recorded in a Microflex MALDI-TOF Bruker spectrometer, and ESI mass spectra were recorded on a HP-5989B API-Electrospray mass spectrometer with S9987A interface. ¹H, ¹³C, and ¹⁹F NMR spectra were recorded on a Bruker AVANCE 400 instrument in the appropriate solvent for each compound. Chemical shifts are quoted relative to SiMe₄ (external) for ¹H and ¹³C and CFCl₃ for ¹⁹F. The quantitative monitoring of the reaction was performed by gas chromatography using a Hewlett-Packard G1800B GCD system, equipped with a Teknokroma TRB-1 cross-linked dimethylpolysiloxane column (30 m × 0.25 mm × 0.25 μm) and MS detector (electron impact with single quadrupole filter). A split injection system with a split ratio of 50:1 was used with helium as carrier gas at a head pressure of 16 psi. Temperature programming was 80 °C (2 min), 20 °C/min, 240 °C (10 min). The inlet temperature was 225 °C and the detector temperature was 250 °C. Conversion of the starting material and product yield were measured by integrating the chromatographic peaks of phenylacetylene (retention time 2.51 min) and acetophenone (retention time 4.17 min). No internal or external standard was used, since both compounds showed a similar response factor ($K_{\text{acetophenone}}/K_{\text{phenylacetylene}} = 1.02$).

[AuCl₂(S₂CNEt₂)] (1). To a solution of [AuCl(tht)] (348 mg, 1.086 mmol) in acetone (30 mL) was added an excess of Cl₂ in CCl₄ solution (5 mL) at room temperature. The mixture was stirred for 30 min, and then NaS₂CNEt₂·3H₂O (245 mg, 1.088 mmol) was added, leading to an orange solution. After 7 h of stirring the solution was

concentrated to 3 mL and, upon addition of 20 mL of hexane, [AuCl₂(S₂CNEt₂)] precipitated as an orange solid, which was subsequently washed with water, isopropyl alcohol, and hexane.

Yield: 88%. Anal. Calcd for **1** (C₅H₁₀AuCl₂NS₂): C, 14.43; H, 2.42; N, 3.37; S, 15.41. Found: C, 14.71; H, 2.56; N, 3.63; S, 15.24. ¹H NMR (400 MHz, 298 K, acetone): 3.94 (q, 2H, CH₂), 1.43 ppm (t, 3H, CH₃). ¹³C{¹H} NMR (101 MHz, 298 K, acetone): 195.6 (S₂CN), 47.8 (CH₂), 12.5 ppm (CH₃). FT-IR (Nujol mull): 1578 cm⁻¹ ν(C–N), 1007 cm⁻¹ ν(CS₂), 365 cm⁻¹, 335 cm⁻¹ ν(Au–Cl). MS (MALDI +): *m/z* 437.878 {[AuCl₂(S₂CNEt₂)] + Na}⁺.

[AuCl₂(S₂CNBn₂)] (2). To a solution of [AuCl(tht)] (86 mg, 0.268 mmol) in CH₂Cl₂ (25 mL) was added an excess of Cl₂ in CCl₄ solution (5 mL) at room temperature. The mixture was stirred for 30 min, and then NaS₂CNBn₂ (79 mg, 0.269 mmol) was added, leading to a yellow solution. After 7 h of stirring the solution was concentrated to 3 mL and, upon addition of 20 mL of hexane, [AuCl₂(S₂CNBn₂)] precipitated as a yellow solid, which was subsequently washed with water, isopropyl alcohol, and hexane.

Yield: 83%. Anal. Calcd for **2** (C₁₃H₁₄AuCl₂NS₂): C, 33.35; H, 2.61; N, 2.59; S, 11.87. Found: C, 33.02; H, 2.56; N, 2.43; S, 11.52. ¹H NMR (400 MHz, 298 K, CD₂Cl₂): 7.45 (m, 3H, C₆H₅), 7.25 (m, 2H, C₆H₅), 4.73 ppm (s, 2H, CH₂). ¹³C{¹H} NMR (101 MHz, 298 K, CD₂Cl₂): 195.8 (S₂CN), 131.1–129.4 (C₆H₅), 53.2 ppm (CH₂). FT-IR (Nujol mull): 1559 cm⁻¹ ν(C–N), 1079 cm⁻¹ ν(CS₂), 346 cm⁻¹, 325 cm⁻¹ ν(Au–Cl). MS (MALDI +): *m/z* 561.973 {[AuCl₂(S₂CNBn₂)] + Na}⁺.

[AuCl₂(S₂CN(Me)Ph)] (3). To a solution of [AuCl(tht)] (361 mg, 1.127 mmol) in CH₂Cl₂ (25 mL) was added an excess of Cl₂ in CCl₄ solution (5 mL) at room temperature. The mixture was stirred for 30 min, and then NaS₂CN(Me)Ph·3H₂O (293 mg, 1.128 mmol) was added, leading to a dark green solution that became orange after 3 h of

stirring. After 7 h of stirring the solution was concentrated to 3 mL and, upon addition of 20 mL of hexane, $[\text{AuCl}_2(\text{S}_2\text{CN}(\text{Me})\text{Ph})]$ precipitated as an orange solid, which was subsequently washed with water, isopropyl alcohol, and hexane.

Yield: 81%. Anal. Calcd for 3 ($\text{C}_6\text{H}_5\text{AuCl}_2\text{NS}_2$): C, 21.34; H, 1.79; N, 3.11; S, 14.25. Found: C, 21.61; H, 1.62; N, 3.21; S, 14.31. ^1H NMR (400 MHz, 298 K, CD_2Cl_2): 7.62 (m, 3H, C_6H_5), 7.35 (m, 2H, C_6H_5), 3.70 ppm (s, 3H, CH_3). $^{13}\text{C}\{^1\text{H}\}$ NMR (101 MHz, 298 K, CD_2Cl_2): 197.9 (S_2CN), 138.3–126.0 (C_6H_5), 41.9 ppm (CH_3). FT-IR (Nujol mull): 1543 cm^{-1} $\nu(\text{C}-\text{N})$, 1070 cm^{-1} $\nu(\text{CS}_2)$, 341 cm^{-1} , 314 cm^{-1} $\nu(\text{Au}-\text{Cl})$. MS (MALDI+): m/z 471.959 $\{[\text{AuCl}_2(\text{S}_2\text{CN}(\text{Me})\text{Ph})] + \text{Na}\}^+$.

$[\text{AuCl}_2(\text{S}_2\text{CN}(\text{pyrrolidine}))]$ (4). To a solution of $[\text{AuCl}(\text{tht})]$ (335 mg, 1.046 mmol) in acetone (30 mL) was added 178 mg of $\text{Na}_2\text{CN}(\text{pyrrolidine})$ (1.049 mmol) at room temperature, leading to a brown solution. After 7 h of stirring, a solid was formed and separated by filtration. The solid was washed with water, isopropyl alcohol, and hexane. This solid was suspended in CH_2Cl_2 , and an excess of Cl_2 in CCl_4 solution (5 mL) was added at room temperature. After 2 h of stirring the solution was concentrated to 3 mL and, upon addition of 20 mL of hexane, $[\text{AuCl}_2(\text{S}_2\text{CN}(\text{pyrrolidine}))]$ precipitated as an orange solid.

Yield: 75%. Anal. Calcd for 4 ($\text{C}_5\text{H}_8\text{AuCl}_2\text{NS}_2$): C, 14.50; H, 1.95; N, 3.38; S, 15.49. Found: C, 14.30; H, 1.71; N, 3.33; S, 15.22. ^1H NMR (400 MHz, 298 K, CD_2Cl_2): 3.78 (m, 2H, $\text{N}-\text{CH}_2$), 2.18 ppm (m, 2H, CH_2). $^{13}\text{C}\{^1\text{H}\}$ NMR (101 MHz, 298 K, CD_2Cl_2): 51.1 ($\text{N}-\text{CH}_2$), 24.4 ppm (CH_2). FT-IR (Nujol mull): 1585 cm^{-1} $\nu(\text{C}-\text{N})$, 1034 cm^{-1} $\nu(\text{CS}_2)$, 341 cm^{-1} , 313 cm^{-1} $\nu(\text{Au}-\text{Cl})$. MS (MALDI+): m/z 435.951 $\{[\text{AuCl}_2(\text{S}_2\text{CN}(\text{pyrrolidine}))] + \text{Na}\}^+$.

General Procedure for the Preparation of $[\text{AuX}_2(\text{S}_2\text{CNET}_2)]$ (X = Br (5), I (6)). To a solution of $[\text{AuCl}_2(\text{S}_2\text{CNET}_2)]$ (1; 40 mg, 0.0961 mmol) in CH_2Cl_2 (20 mL) was added a solution of NaX (X = Cl, Br, I) in water (20 mL) at room temperature. The mixture was stirred for 16 h, and then, the organic layer was separated and dried with anhydrous MgSO_4 . The solution was concentrated to 3 mL and, upon addition of 20 mL of hexane, $[\text{AuX}_2(\text{S}_2\text{CNET}_2)]$ precipitated as an orange solid (5) or a dark red solid (6).

$[\text{AuBr}_2(\text{S}_2\text{CNET}_2)]$ (5). Yield: 93%. Anal. Calcd for 5 ($\text{C}_5\text{H}_{10}\text{AuBr}_2\text{NS}_2$): C, 11.89; H, 2.00; N, 2.77; S, 12.70. Found: C, 11.62; H, 2.26; N, 3.01; S, 12.92. ^1H NMR (400 MHz, 298 K, CDCl_3): 3.68 (q, 2H, CH_2), 1.41 ppm (t, 3H, CH_3). $^{13}\text{C}\{^1\text{H}\}$ NMR (101 MHz, 298 K, CDCl_3): 194.9 (S_2CN), 45.7 (CH_2), 12.5 ppm (CH_3). FT-IR (Nujol mull): 1576 cm^{-1} $\nu(\text{C}-\text{N})$, 995 cm^{-1} $\nu(\text{CS}_2)$. MS (ESI-): m/z 505.801 $\{[\text{AuBr}_2(\text{S}_2\text{CNET}_2)] + \text{H}\}^-$.

$[\text{AuI}_2(\text{S}_2\text{CNET}_2)]$ (6). Yield: 91%. Anal. Calcd for 6 ($\text{C}_5\text{H}_{10}\text{AuI}_2\text{NS}_2$): C, 10.02; H, 1.68; N, 2.34; S, 10.71. Found: C, 10.27; H, 1.75; N, 2.55; S, 10.58. ^1H NMR (400 MHz, 298 K, CDCl_3): 3.61 (q, 2H, CH_2), 1.39 ppm (t, 3H, CH_3). $^{13}\text{C}\{^1\text{H}\}$ NMR (101 MHz, 298 K, CDCl_3): 198.3 (S_2CN), 44.6 (CH_2), 12.5 ppm (CH_3). FT-IR (Nujol mull): 1559 cm^{-1} $\nu(\text{C}-\text{N})$, 997 cm^{-1} $\nu(\text{CS}_2)$. MS (ESI-): m/z 599.769 $\{[\text{AuI}_2(\text{S}_2\text{CNET}_2)] + \text{H}\}^-$.

$[\text{Au}(\text{C}_6\text{F}_5)_2(\text{S}_2\text{CNET}_2)]$ (7). To a solution of $[\text{Au}(\text{C}_6\text{F}_5)_2\text{Cl}]_2$ (128 mg, 0.113 mmol) in acetone (15 mL) was added $\text{Na}_2\text{S}_2\text{CNET}_2 \cdot 3\text{H}_2\text{O}$ (51 mg, 0.226 mmol) at room temperature and under an Ar atmosphere, leading to a light brown solution. After 2 h of stirring the mixture was filtered off. The remaining solution was concentrated to 3 mL and, upon addition of 20 mL of hexane, $[\text{Au}(\text{C}_6\text{F}_5)_2(\text{S}_2\text{CNET}_2)]$ precipitated as a light brown solid.

Yield: 85%. Anal. Calcd for 7 ($\text{C}_{17}\text{H}_{10}\text{AuF}_{10}\text{NS}_2$): C, 30.06; H, 1.48; N, 2.06; S, 9.44. Found: C, 30.22; H, 1.77; N, 2.27; S, 9.37. ^1H NMR (400 MHz, 298 K, acetone): 3.90 (q, 2H, CH_2), 1.42 ppm (t, 3H, CH_3). $^{13}\text{C}\{^1\text{H}\}$ NMR (101 MHz, 298 K, acetone): 197.8 (S_2CN), 147.4–110.0 (C_6F_5), 46.8 (CH_2), 12.4 ppm (CH_3). ^{19}F NMR (377 MHz, 298 K, acetone): -122.1 (m, 4F, F_{ortho}), -158.5 (t, 2F, F_{para}), -163.2 ppm (m, 4F, F_{meta}). FT-IR (Nujol mull): 1532 cm^{-1} $\nu(\text{C}-\text{N})$, 1064 cm^{-1} $\nu(\text{CS}_2)$, 1503 cm^{-1} , 968 cm^{-1} , 795 cm^{-1} $\nu(\text{C}_6\text{F}_5)$. MS (ESI+): m/z 701.952 $\{[\text{Au}(\text{C}_6\text{F}_5)_2(\text{S}_2\text{CNET}_2)] + \text{Na}\}^+$.

Crystallography. Crystals were mounted in inert oil on a glass fiber and transferred into the cold gas stream of an Oxford Cryosystems open-flow cryostat mounted on a Nonius Kappa CCD

diffractometer. Data were collected at -100 °C using graphite-monochromated Mo $K\alpha$ radiation ($\lambda = 0.71073$ Å). The scan types were ω and ϕ . Absorption correction: semiempirical (based on multiple scans). The structures were solved by Patterson methods and refined on F^2 using the program SHELXL97.⁴⁷ All non-hydrogen atoms were refined anisotropically. Crystal data for 2: $\text{C}_{15}\text{H}_{14}\text{AuCl}_2\text{NS}_2$, monoclinic, $C2/c$, $a = 17.5767(16)$ Å, $b = 12.0983(12)$ Å, $c = 8.1859(6)$ Å, $\beta = 109.339(5)^\circ$, $V = 1642.5(3)$ Å³, $Z = 4$, $\mu = 9.527$ mm⁻¹, 12032 reflections, $2\theta_{\text{max}} = 55^\circ$, 1864 unique ($R_{\text{int}} = 0.0714$), $R = 0.0312$, $R_w = 0.0666$ for 97 parameters, no restrictions, $S = 1.055$, maximum $\Delta\rho = 2.607$ e Å⁻³. The crystal structure of complex 2 is shown in Figure 1. CCDC-975565 contains the supplementary crystallographic data for this paper. These data can be obtained free of charge via www.ccdc.cam.ac.uk/conts/retrieving.html (or from the Cambridge Crystallographic Data Centre, 12 Union Road, Cambridge CB2 1EZ, UK; fax, (+44) 1223-336-033; e-mail, deposit@ccdc.cam.ac.uk).

Computational Details. All geometry optimizations were carried out using the M06-2X hybrid functional.⁴⁸ In all calculations, the heteroatoms were treated by SDD pseudopotentials,⁴⁹ including only the valence electrons for each atom. For these atoms double- ζ basis sets were used, augmented with d-type polarization functions.⁵⁰ For H atoms, a double- ζ basis set was used, together with a p-type polarization function.⁵¹ The 19-valence-electron SDD pseudopotential⁵² was employed for Au atoms, together with two f-type polarization functions.⁵³ Full geometry optimizations and transition structure (TS) searches were carried out with the Gaussian 09 package.⁵⁴ The possibility of different conformations was taken into account for all structures. Frequency analyses were carried out at the same level used in the geometry optimizations, and the nature of the stationary points was determined in each case according to the appropriate number of negative eigenvalues of the Hessian matrix. Scaled frequencies were not considered. Mass-weighted intrinsic reaction coordinate (IRC) calculations were carried out by using the Gonzalez and Schlegel scheme^{55,56} in order to ensure that the TSs indeed connected the appropriate reactants and products. Bulk solvent effects were considered implicitly by performing single-point energy calculations on the gas-phase optimized geometries, through the IEFPCM polarizable continuum model⁵⁷ as implemented in Gaussian 09. The internally stored parameters for dichloromethane were used to calculate solvation free energies (ΔG_{sol}). Gibbs free energies (ΔG) were used for the discussion on the relative stabilities of the considered structures. The Au–X bond dissociation energies were estimated using counterpoise correction for the basis set superposition error (BSSE).⁵⁸ Cartesian coordinates, electronic energies, entropies, enthalpies, Gibbs free energies, and lowest frequencies of the different conformations of all structures considered are available as Supporting Information.

■ ASSOCIATED CONTENT

Supporting Information

Tables, figures, and CIF and xyz files giving spectroscopic characterization of all new compounds, crystal structure data, and computational data. This material is available free of charge via the Internet at <http://pubs.acs.org>.

■ AUTHOR INFORMATION

Corresponding Author

*E-mail for J.M.L.: josemaria.lopez@unirioja.es.

Notes

The authors declare no competing financial interest.

■ ACKNOWLEDGMENTS

The DGI (MEC)/FEDER (project number CTQ 2013-48635-C2-2) is acknowledged for financial support. J.C. also acknowledges the MEC for a FPU grant. We gratefully thank CESGA for computer support.

REFERENCES

- (1) Hashmi, A. S. K.; Hutchings, G. J. *Angew. Chem., Int. Ed.* **2006**, *45*, 7896.
- (2) Gorin, D. J.; Toste, F. D. *Nature* **2007**, *446*, 395.
- (3) Jimenez-Nunez, E.; Echavarren, A. M. *Chem. Commun.* **2007**, 333.
- (4) Hashmi, A. S. K.; Rudolph, M. *Chem. Soc. Rev.* **2008**, *37*, 1766.
- (5) Hintermann, L.; Labonne, A. I. *Synthesis* **2007**, *8*, 1121.
- (6) Budde, W. L.; Dessy, R. E. *J. Am. Chem. Soc.* **1963**, *85*, 3964.
- (7) Uemura, S.; Miyoshi, H.; Okano, M. *J. Chem. Soc., Perkin Trans. 1* **1980**, 1098.
- (8) James, B. R.; Rempel, G. L. *J. Am. Chem. Soc.* **1969**, *91*, 863.
- (9) Francisco, L. W.; Moreno, D. A.; Atwood, J. D. *Organometallics* **2001**, *20*, 4237.
- (10) Mizushima, E.; Sato, K.; Hayashi, T.; Tanaka, M. *Angew. Chem., Int. Ed.* **2002**, *41*, 4563.
- (11) Ibrahim, N.; Vilhelmsen, M. H.; Pernpointner, M.; Rominger, F.; Hashmi, A. S. K. *Organometallics* **2013**, *32*, 2576.
- (12) Czégéni, C. E.; Papp, G.; Kathó, Á.; Joó, F. *J. Mol. Catal. A: Chem.* **2011**, *340*, 1.
- (13) Nun, P.; Ramón, R. S.; Gaillard, S.; Nolan, S. P. *J. Organomet. Chem.* **2011**, *696*, 7.
- (14) Gaillard, S.; Bosson, J.; Ramón, R. S.; Nun, P.; Slawin, A. M. Z.; Nolan, S. P. *Chem. Eur. J.* **2010**, *16*, 13729.
- (15) Gómez-Suárez, A.; Oonishi, Y.; Meiries, S.; Nolan, S. P. *Organometallics* **2013**, *32*, 1106.
- (16) de Frémont, P.; Singh, R.; Stevens, E. D.; Petersen, J. L.; Nolan, S. P. *Organometallics* **2007**, *26*, 1376.
- (17) Lein, M.; Rudolph, M.; Hashmi, S. K.; Schwerdtfeger, P. *Organometallics* **2010**, *29*, 2206.
- (18) Hashmi, A. S. K. *Chem. Rev.* **2007**, *107*, 3180.
- (19) Corma, A.; Leyva-Pérez, A.; Sabater, M. J. *Chem. Rev.* **2011**, *111*, 1657.
- (20) Marion, N.; Nolan, S. P. *Chem. Soc. Rev.* **2008**, *37*, 1776.
- (21) Nolan, S. P. *Acc. Chem. Res.* **2011**, *44*, 91.
- (22) Teles, J. H.; Brode, S.; Chabanas, M. *Angew. Chem., Int. Ed.* **1998**, *37*, 1415.
- (23) Casado, R.; Contel, M.; Laguna, M.; Romero, P.; Sanz, S. *J. Am. Chem. Soc.* **2003**, *125*, 11925.
- (24) Leyva, A.; Corma, A. *J. Org. Chem.* **2009**, *74*, 2067.
- (25) Marion, N.; Ramón, R. S.; Nolan, S. P. *J. Am. Chem. Soc.* **2008**, *131*, 448.
- (26) Krauter, C. M.; Hashmi, A. S. K.; Pernpointner, M. *ChemCatChem* **2010**, *2*, 1226.
- (27) Mazzone, G.; Russo, N.; Sicilia, E. *Organometallics* **2012**, *31*, 3074.
- (28) Fukuda, Y.; Utimoto, K. *J. Org. Chem.* **1991**, *56*, 3729.
- (29) Teles, J. H. In *Modern Gold Catalyzed Synthesis*; Wiley-VCH: Weinheim, Germany, 2012; p 201.
- (30) Gimeno, M. C.; Laguna, A. In *Comprehensive Coordination Chemistry II*; McCleverty, J. A., Meyer, T. J., Eds.; Pergamon: Oxford, U.K., 2003; p 911.
- (31) Bojan, V. R.; López-de-Luzuriaga, J. M.; Manso, E.; Monge, M.; Olmos, M. E. *Organometallics* **2011**, *30*, 4486.
- (32) Onwudiwe, D. C.; Ajibade, P. A. *Int. J. Mol. Sci.* **2011**, *12*, 1964.
- (33) Usón, R.; Laguna, A.; Vicente, J. *Rev. Acad. Cienc. Zaragoza* **1976**, *3*, 211.
- (34) Uson, R.; Laguna, A.; Laguna, M.; Manzano, B. R.; Jones, P. G.; Sheldrick, G. M. *J. Chem. Soc., Dalton Trans.* **1984**, 285.
- (35) Jian, F.; Lu, L.; Wang, X.; Shanmuga Sundara Raj, S.; Razak, I. A.; Fun, H.-K. *Acta Crystallogr., Sect. C* **2000**, *56*, 939.
- (36) Parish, R. V.; Howe, B. P.; Wright, J. P.; Mack, J.; Pritchard, R. G.; Buckley, R. G.; Elsome, A. M.; Fricker, S. P. *Inorg. Chem.* **1996**, *35*, 1659.
- (37) Lock, C. J. L.; Turner, M. A.; Parish, R. V.; Potter, G. *Acta Crystallogr., Sect. C* **1988**, *44*, 2082.
- (38) Carlson, T. F.; Watson, W. H. *Private communication to the Cambridge Structural Database*, deposition number CCDC 160743.
- (39) Vicente, J.; Chicote, M.-T.; González-Herrero, P.; Jones, P. G. *Inorg. Chem.* **1997**, *36*, 5735.
- (40) Jentsch, D.; Jones, P. G.; Thone, C.; Schwarzmann, E. *J. Chem. Soc., Chem. Commun.* **1989**, 1495.
- (41) Vicente, J.; Chicote, M. T.; González-Herrero, P.; Jones, P. G.; Humphrey, M. G.; Cifuentes, M. P.; Samoc, M.; Luther-Davies, B. *Inorg. Chem.* **1999**, *38*, 5018.
- (42) Saggioro, D.; Rigobello, M. P.; Paloschi, L.; Folda, A.; Moggach, S. A.; Parsons, S.; Ronconi, L.; Fregona, D.; Bindoli, A. *Chem. Biol.* **2007**, *14*, 1128.
- (43) Schmidbaur, H.; Schier, A. *Chem. Soc. Rev.* **2008**, *37*, 1931.
- (44) Allen, E. A.; Wilkinson, W. *Spectrochim. Acta, Part A* **1972**, *28*, 2257.
- (45) Usón, R.; Laguna, A.; Laguna, M.; Abad, M. *J. Organomet. Chem.* **1983**, *249*, 437.
- (46) Manav, N.; Mishra, A. K.; Kaushik, N. K. *Spectrochim. Acta, Part A* **2006**, *65*, 32.
- (47) Sheldrick, G. M. *SHELXL97, Program for Crystal Structure Refinement*; University of Göttingen, Göttingen, Germany, 1997.
- (48) Zhao, Y.; Truhlar, D. *Theor. Chem. Acc.* **2008**, *120*, 215.
- (49) Bergner, A.; Dolg, M.; Küchle, W.; Stoll, H.; Preuß, H. *Mol. Phys.* **1993**, *80*, 1431.
- (50) Huzinaga, S.; Andzelm, J. *Gaussian basis sets for molecular calculations*; Elsevier: Amsterdam, 1984.
- (51) Huzinaga, S. *J. Chem. Phys.* **1965**, *42*, 1293.
- (52) Andrae, D.; Häußermann, U.; Dolg, M.; Stoll, H.; Preuß, H. *Theor. Chim. Acta* **1990**, *77*, 123.
- (53) Pyykkö, P.; Runeberg, N.; Mendizabal, F. *Chem. Eur. J.* **1997**, *3*, 1451.
- (54) Frisch, M. J.; Trucks, G. W.; Schlegel, H. B.; Scuseria, G. E.; Robb, M. A.; Cheeseman, J. R.; Scalmani, G.; Barone, V.; Mennucci, B.; Petersson, G. A.; Nakatsuji, H.; Caricato, M.; Li, X.; Hratchian, H. P.; Izmaylov, A. F.; Bloino, J.; Zheng, G.; Sonnenberg, J. L.; Hada, M.; Ehara, M.; Toyota, K.; Fukuda, R.; Hasegawa, J.; Ishida, M.; Nakajima, T.; Honda, Y.; Kitao, O.; Nakai, H.; Vreven, T.; Montgomery, J. A., Jr.; Peralta, J. E.; Ogliaro, F.; Bearpark, M.; Heyd, J. J.; Brothers, E.; Kudin, K. N.; Staroverov, V. N.; Kobayashi, R.; Normand, J.; Raghavachari, K.; Rendell, A.; Burant, J. C.; Iyengar, S. S.; Tomasi, J.; Cossi, M.; Rega, N.; Millam, J. M.; Klene, M.; Knox, J. E.; Cross, J. B.; Bakken, V.; Adamo, C.; Jaramillo, J.; Gomperts, R.; Stratmann, R. E.; Yazyev, O.; Austin, A. J.; Cammi, R.; Pomelli, C.; Ochterski, J. W.; Martin, R. L.; Morokuma, K.; Zakrzewski, V. G.; Voth, G. A.; Salvador, P.; Dannenberg, J. J.; Dapprich, S.; Daniels, A. D.; Farkas, Ö.; Foresman, J. B.; Ortiz, J. V.; Cioslowski, J.; Fox, D. J. *Gaussian 09, Revision A.02*; Gaussian, Inc., Wallingford, CT, 2009.
- (55) Gonzalez, C.; Schlegel, H. B. *J. Chem. Phys.* **1989**, *90*, 2154.
- (56) Gonzalez, C.; Schlegel, H. B. *J. Phys. Chem.* **1990**, *94*, 5523.
- (57) Scalmani, G.; Frisch, M. J. *J. Chem. Phys.* **2010**, *132*.
- (58) Boys, S. F.; Bernardi, F. *Mol. Phys.* **1970**, *19*, 553.